African Journal of Biology and Medical Research
ISSN: 2689-534X
Volume 4, Issue 4, 2021 (pp. 8-21)
www.abjournals.org

THE POTENTIAL EFFECT OF SILVER NANOPARTICLES ON THE EXPRESSION AND LEVELS OF SKIN MATRIX METALLOPROTEINASES (GELATINASES): IN VIVO ASSESSMENT

Sameh Mohamed Abouzead[1], Abdelmordy M. Mohamed[2], Ahmed R. Ezzat[3] and Gamal M. Morsy[4]

[1]Chief Manager of the Biology Department, Technical Research Center, Cairo, Egypt
E-mail: samehzead77@gmail.com

[2]Professor of Genetics and Molecular Biology, Zoology Department, Faculty of Science, Ain Shams University, Cairo, Egypt

[3]Professor of Physiology, Zoology Department, Faculty of Science, Ain Shams University, Cairo, Egypt

[4]Professor of Toxicology, Zoology Department-Faculty of Science, Cairo University, Giza, Egypt

Cite this article:

Sameh M.A., Abdelmordy M.M., Ahmed R.E., Gamal M.M. (2021), The Potential Effect of Silver Nanoparticles on the Expression and Levels of Skin Matrix Metalloproteinases (Gelatinases): In Vivo Assessment. African Journal of Biology and Medical Research 4(4), 8-21. DOI: 10.52589/AJBMR-QMDCSAYF.

Manuscript History

Received: 3 Nov 2021

Accepted: 29 Nov 2021

Published: 13 Dec 2021

ABSTRACT: *The current work aimed to investigate the enzymatic activities and the expression profiles of the metalloproteinases MMP-2 and MMP-9 in the skin of rabbits as an animal model, upon sub-acute dermal exposure to Ag-NPs. This was done in order to determine their potential effect on these proteolytic enzymes which have been traditionally involved in many physiological processes such as inflammation and wound healing which are among the main applications Ag-NPs containing medical products. The rabbits were topically exposed to every other day dose of 0.5% Ag-NPs for 7- and 14-days experimental periods. Both periods were followed by 7 days recovery time. The results revealed the remarkable effect of Ag-NPs on MMPs at both the enzyme production and the transcriptional levels. The effect was time dependent where no significant changes were found after the 7 days of exposure, while the concentrations of MMP-2 and MMP-9 as well as the expression of their encoding genes were significantly elevated in the skin of the exposure and recovery groups at the 14 days experimental period. MMP-9 was the most affected enzyme, whereas MMP-2 showed the minimal effect. Several mechanisms and pathways have been suggested to explain the disturbance of MMPs which require further molecular studies to obtain more evidence supporting the most probable explanation.*

KEYWORDS: Silver Nanoparticles, Matrix Metalloproteinase, Gelatinase, Wound Healing.

Article DOI: 10.52589/AJBMR-QMDCSAYF
DOI URL: https://doi.org/10.52589/AJBMR-QMDCSAYF

INTRODUCTION

Nanotechnology is a rapidly growing field of science which involves the control and manipulation of matter at the nanoscale. The emergence of this innovative technology offers great promises in various fields to improve higher quality products. It is noteworthy that silver nanoparticles (Ag-NPs) have occupied a significant position and are gaining a high popularity among other metal nanomaterials (NMs). Their based products represent one of the fastest growing categories in the current market and are being used in a variety of applications (Lee and Jun, 2019).

Ag-NPs are fine particles of metallic silver that have at least one dimension less than 100 nm (Koduru *et al*., 2018). At this scale, the surface area to volume ratio of these particles becomes large enough for establishing new physicochemical properties to be acquired as well as completely different biological behaviour (Mikhailova, 2020). In general, the exceptional popularity of Ag-NPs relies on the fact that, they have an effective bactericidal activity against a broad spectrum of gram-negative and positive bacteria (Yin *et al*., 2020) as well as a fast-acting fungicidal against a broad spectrum of fungi (Mussin *et al*., 2019). Moreover, Ag-NPs dressings have been shown to possess an anti-inflammatory activity (El-Rafie *et al*., 2017), accelerate wound healing process (Paladini and Pollini, 2019) and even inhibit viral replication (Panja *et al*., 2021).

Since the medical use of Ag-NPs in wound dressings and surgical meshes represents a prominent area in their applications, attention has been given to their potential ability for modifying skin matrix metalloproteinases (MMPs). The progressive awareness of MMPs, which are zinc-dependent proteolytic enzymes have been traditionally associated with their role in the degradation and turnover of numerous components of the extracellular matrix (ECM). Recent reports have shown that MMPs are directly implicated in almost every biological process involving matrix remodelling to cell death or necrosis throughout the mammalian life span (Velnar and Gradisnik, 2018). Moreover, MMPs play a primary role in normal tissue maintenance and functions including wound healing, tissue repair, immune defence, inflammation, neoangiogenesis and apoptosis (Negut *et al*., 2018).

Currently, up to 23 types of MMPs have been identified in humans. The structure of all MMPs family members is closely similar, where a zinc-binding motif is included in the catalytic domain central core. MMPs can be categorized into subgroups according to their structure and substrate specificity including: collagenases, gelatinases, stromelysins, matrilysins, and membrane type MMPs (Hrabia, 2021). In the skin, MMP-2 (Gelatinase A) and MMP-9 (Gelatinase B) are the most prominent and well defined MMPs. They are responsible for degrading several ECM components such as gelatine, elastin, fibronectin as well as collagen (Nyman *et al*., 2011; Gou *et al*., 2020).

A considerable number of studies have explored the efficiency of Ag-NPs in accelerating the wound healing process, but to our knowledge the exact mode of action has not been investigated in details *in vivo* studies to disclose the role of Ag-NPs in modulating skin MMPs, which are essential for the healing process. Accordingly, the present work was designed to investigate the potential effect of Ag-NPs on the MMP-2 and MMP-9 enzyme production in conjunction with their gene expression pattern. Rabbits were selected as an animal model of study while the topical application was chosen as the skin represents the main exposure route to Ag-NPs based products, especially in the medical applications.

Article DOI: 10.52589/AJBMR-QMDCSAYF
DOI URL: https://doi.org/10.52589/AJBMR-QMDCSAYF

METHODOLOGY

Preparation of Silver Nanoparticles

Silver Nanoparticles (Ag-NPs) were obtained from Skyspring Nanomaterials, Inc. (Houston, USA). The NPs shape was relatively spherical, with an average size of 10 to 15nm, and a purity of 99.9%, as reported by the manufacturer. The ultrasonication of Ag-NPs was important to facilitate the processes of characterization and the exposure to Ag metal, during the experiments. In order to prepare a homogeneous aqueous suspension containing a concentration of 0.5% silver, a half gram of Ag-NPs was added to 100 ml of deionized water. Then the aqueous suspension was ultra-sonicated for 20 to 30 min using a Misonix-4000, ultrasonic homogenizer.

Characterization of Silver Nanoparticles

X-ray Fluorescence Analysis

The purity of Ag-NPs was examined using S2 RANGER energy dispersive X-ray fluorescence (EDXRF) spectrometer (Bruker, GmbH. Germany). The Ag-NPs were placed in aluminium beads for generating disc pellets using a manual presser device. The elemental analysis was performed automatically at 50-Watt power. The obtained spectrum was analyzed using "EQUA ALL" software using multi-element standards in the XRF library. The data processing and quantitative results were obtained at the same time with the standard X-Flash software.

Transmission Electron Microscopy

The shape, size, and aggregation behaviour of the ultrasonicated Ag-NPs were examined using the high-resolution Transmission Electron Microscopy (TEM) technique. The analysis was applied by the aid of JEM1400-plus TEM (JEOL, Japan) with an acceleration voltage of 100 kV and a magnification range up to 48000x. Carbon coated 200 mesh copper grids were pre-treated with 20µl of poly-L-lysine 0.01 % (w/v) for 15 min. The grids were washed twice, then 3µl of the ultrasonicated Ag-NPs suspension were dropped into the grids for 5 min and then rinsed with 3µl of 2-propanol. The grids were allowed to dry overnight at room temperature in a covered crystallizing dish. Images of the selected regions were taken using the built-in high resolution (7768 x 7768) lens-coupled AMT XR41-B 8-megapixel camera where a minimum of about 100 Ag-NPs were considered. The particle size analysis and distribution uniformity were processed using the capture JENIE-X viewer software.

The Experimental Animals

The healthy adult male New Zealand white rabbits, *Oryctolagus cuniculus*, with an average body weight of 2.1 ± 0.1 kg were used as an experimental mammalian model. Rabbits were purchased from the Military Animal Farm (Nasr City, Cairo, Egypt). The rabbits were acclimatized seven days prior to the initiation of the experiments, in accordance with the international guideline principles for the care and use of laboratory animals in scientific research (NRC, 2011). They were housed individually in steel cages embedded with sawdust at a temperature of 21°±2°C, relative humidity of 40% to 50%, and cyclic daylight of 12 h/day. Rabbits had access to water and a balanced commercial pellet diet *ad libitum*. The

Article DOI: 10.52589/AJBMR-QMDCSAYF
DOI URL: https://doi.org/10.52589/AJBMR-QMDCSAYF

food debris and faeces were removed from the cages, which were cleaned daily to keep the sawdust dry throughout the course of experiments.

The Experimental Design

The current work was designed to evaluate the effect of sub-acute exposure to Ag-NPs in two different experimental periods (EP; 7 and 14 days). The suitable number of animals was calculated using the G-Power analysis (version 3.1.9.7) and was found to be thirty rabbits (N=30). The thirty rabbits were divided into three equal groups (n=10). The rabbits of group (I) were topically exposed to water and served as control, whereas groups (II) and (III) were exposed to 1ml of 0.5% Ag-NPs every other day, for 7 and 14 days, respectively. The current experimental concentration was chosen below the toxic dose of Ag-NPs, which was estimated by similar preliminary studies (Korani *et al*., 2011; Korani *et al*., 2013). After seven and fourteen days of exposure, rabbits of groups II (exposure group) were sacrificed and quickly dissected to obtain the skin. On the other hand, rabbits of group III (recovery group) were sacrificed after seven days from the end of each exposure period (Table 1).

Table 1: The full constructed experimental design of sub-acute experimentation.

Sources	Group I (Control)		Group II (Exposure)		Group III (Recovery)	
Sampling time	7 days	14 days	7 days	14 days	7 days	7 days
Deionized H2O	1 ml	1 ml	----	----	----	----
Ag-NPs (0.5%)	----	----	1 ml	1 ml	1 ml	1 ml
Sample Size (n)	5	5	5	5	5	5
No. of exposure	Every other day					

Animals Preparation and Sampling

Each rabbit dorsal back was clipped using an electric clipper supplied with 0.22 mm finishing blade to carefully remove the hair without damaging the skin. An area of 6x6 cm was marked with a water-based FDA approved dye marker where the suspensions of test material were applied. The marked area of the skin was separated and sliced immediately after scarifying. Then one gram of skin tissue was quickly submerged in a RNAlater solution for RNA stabilization to prevent RNA damage, and stored frozen at -80°C for further gene expression analysis. The rest of the skin tissue was immersed in phosphate buffered solution (pH 7.4) containing 0.16 mg/ml heparin to remove the red blood cells and then stored at -80°C until used in measuring the levels of skin MMPs.

Skin Matrix Metalloproteinases Levels

A skin sample (~ 0.5 g) from each rabbit was homogenized in a 9 ml cold buffer (100mM potassium phosphate pH 7, containing 2mM EDTA) and then centrifuged at 5,000 rpm for 5 min at 4°C. The supernatant was collected for assaying using a specific rabbit MMPs-ELISA kits (Elabscience Biotechnology Inc, USA, catalogue number: E-EL-RB1540 and E-EL-RB1997), for the quantitative determination of MMP-2 and MMP-9 levels. The measurement principle was based on using a pre-coated ELISA microplate with an antibody specific to rabbit MMPs. The antibody combined with the target MMP molecule in the sample. The concentration was then calculated from a standard curve according to the measured optical

Article DOI: 10.52589/AJBMR-QMDCSAYF
DOI URL: https://doi.org/10.52589/AJBMR-QMDCSAYF

density (OD). The optical density was measured at 450 nm using a microplate reader model ELx800 from Biotek Instruments, Inc, USA. The average of the duplicate readings (two wells) for each standard and samples was calculated, then a standard curve was created by plotting the mean OD value for each standard against the concentration using the curve expert 1.4 software. The concentrations were finally calculated and expressed as ng/g wt.

Gene Expression Analysis of Matrix Metalloproteinases

The expressions of MMP-2 and MMP-9 were assessed using the End-Point Reverse Transcription Polymerase Chain Reaction (RT-PCR). The total RNA was extracted from the skin samples using the RNeasy Fibrous Tissue Midi Kit (Qiagen Chemicals, Germany, catalogue number 74704). The tissue samples were removed from the RNA*later* and washed with 2ml lysis buffer. Then, 100 mg from each sample were homogenized in 1ml RLT buffer (Guanidine thiocyanate) and 10µl Mercapto-ethanol using tissue lyser for 3 min at 20Hz. Four ml RNase-free water and 65µl proteinase K solutionere added to the lysate and incubated at 55°C for 20 min. The mixture was centrifuged at 3000 rpm for 5 min at room temperature, and the supernatant was collected. Three ml of 100% ethanol were added to the collected supernatant in a clean RN-easy mini spin column, and centrifuged at 25°C for 5 min at 5000 rpm to completely bind the total RNA to the silica membrane. The RN-easy spin column was moved to a new collection tube and spun twice with 150µl RNase-free water. Finally, the purified elute of total RNA was collected (~150 µl for each sample) after3 min of centrifugation at 5000 rpm. The template RNAs were stored at –20°C for quality analysis and reverse transcription.

The quantity and purity of total RNA were evaluated using the NanoDrop 8000 Spectrophotometer by Thermo Fisher Scientific, USA. The instrument determined the RNA concentration in the samples and performed the programmed measurements of A230, A260, and A280. From each RNA sample, 3µl were diluted in 57µl of 10 mM Tris-HCl, pH 7.5 (1:20 dilution) to be ready for analysis. On the other hand, the integrity and size distribution of total RNA were checked using the formaldehyde agarose (FA) gel electrophoresis. Electrophoresis was performed using a 14 x 8cm / 0.7mm Flexicast midi-horizontal unit (Expedeon Ltd., USA) under denaturing conditions. A low running voltage (60-70V) was chosen to avoid trailing and smearing of RNA bands. Total RNA (40µl) was mixed with 10µl of the loading buffer and incubated for 3–5 min at 65°C, chilled on ice, and loaded onto the FA gel. Finally, stained with ethidium bromide solution and visualized for analysis.

The PCR was carried out by using a two-step prime script RT-PCR kit (TaKaRa Bio Inc. Shiga, Japan, catalogue number RR014A) following the manufacturer's protocol. A negative control was amplified with each set of samples to validate the primers and for verifying the residual DNA contamination. PCR was performed for 32 cycles in a Thermocycler T3000 Combi-system (Biometra, Germany). The cycling parameters were: denaturation for 45 s at 93ºC, annealing for 45 s at 58ºC, extension for 1.5 min at 72ºC. Finally, the reaction was finished by a cooling step at 4°C for 1 min. The primers (Rabbit MMP-2 and MMP-9) were chosen, as the only amplified sequences specific to the particular genes. In addition, a housekeeping gene, rabbit glyceraldehyde-3-phosphate dehydrogenase (GAPDH) was used as an internal control.

All primer pairs were designed and supplied by Creative Biogene Biotechnology Inc, USA. The Primers details for MMP-2 were; sense 5'-CATGTCGACTCATGGCGGGA-3' and

Article DOI: 10.52589/AJBMR-QMDCSAYF
DOI URL: https://doi.org/10.52589/AJBMR-QMDCSAYF

antisense 5'-TAACGTTGGTCAGGGCAGAAA-3' (Annealing temperature, 57°C; expected PCR product size, 662bp; Gene Ref. ID, NM001082209). Whereas, for MMP-9, the primers were; sense 5'-ACGGATCCAGTTACCGTTCA-3' and antisense 5'-TGAATACGGCTCCA GTAGCTA-3' (Annealing temperature, 57°C; expected PCR product size, 707bp; Gene Ref. ID, NM001082203), and for GAPDH were; sense 5'-ACGGTGCACGCCATC ACTGC-3' and antisense 5'-TGCTACACGACCATCTTGCGA-3' (Annealing temperature, 59°C; expected PCR product size, 333bp; Gene Ref. ID, NM001082203).

The PCR amplified fragments (6 µl from each sample) were separated on 2% agarose gel and visualized by ethidium bromide staining, then, digitally photographed using Biometra Ti5 Bio Doc system. The organization, size validation and densitometry analysis of photographic images were done using the Bio Doc Analyze 2.1 software (Biometra, Germany). The relative gene expression levels were quantified by normalizing the corresponding intensities of target genes to the stable level of GAPDH as a control (Caroline, 2002; Janssens *et al*., 2004).

Statistical Analysis

G-power analysis was used for the estimation of the total number of animals (N) and the number of animals within groups (n). The data were initially checked for normality by one-sample Shapiro–Wilk test where the null hypothesis was accepted and the calculated data were considered normally distributed when $P \geq 0.05$ (Shapiro and Wilk, 1965).

In order to test the effect of different exposure levels of Ag-NPs on the examined parameters, One-way analysis of variances (ANOVA) was performed. Duncan's post hoc test was carried out for normally distributed samples with homogeneous variances whereas Tukey HSD and Games-Howell tests were used for the heterogeneous sets. Data were expressed as mean ± standard error of the mean (SEM), mean values were considered to be statistically significant at $P< 0.05$. All analyses were performed using the Statistical Package for the Social Sciences (SPSS) software for Windows, version 26.0 by Armonk, IBM Corp. USA.

RESULTS

Characterization of Silver Nanoparticles

The XRF analysis confirmed that elemental silver was the main component which represented 99.9 % percent by weight in the examined Ag-NPs samples. Trivial traces of s impurities including Antimony (Sb), Bismuth (Bi), Ferric (Fe), Zinc (Zn), Copper (Cu), Nickel (Ni) and Cadmium (Cd) were also found. Moreover, no oxides were detected which demonstrated that the sample consisted of pure silver with no oxidation (Table 2).

Article DOI: 10.52589/AJBMR-QMDCSAYF
DOI URL: https://doi.org/10.52589/AJBMR-QMDCSAYF

Table 2. The XRF data analysis shows the elemental composition of the examined Ag-NPs as expressed by the percentage of weight in the sample.

Element	Formula	Weight %
Silver	Ag	99.964
Antimony	Sb	0.0065
Bismuth	Bi	0.0086
Ferric	Fe	0.0076
Zinc	Zn	0.0043
Copper	Cu	0.0074
Nickel	Ni	0.0015
Cadmium	Cd	0.0001

TEM imaging showed that the ultrasonicated Ag-NPs were spherical in shape with a clearly smooth surface. In addition, the particles were homogeneously dispersed in the suspension with no sign of any aggregations. The particle size distribution ranged from 12.2 to 14.9 nm with an average particle diameter of 13.9 ± 0.94 nm (Figure 1).

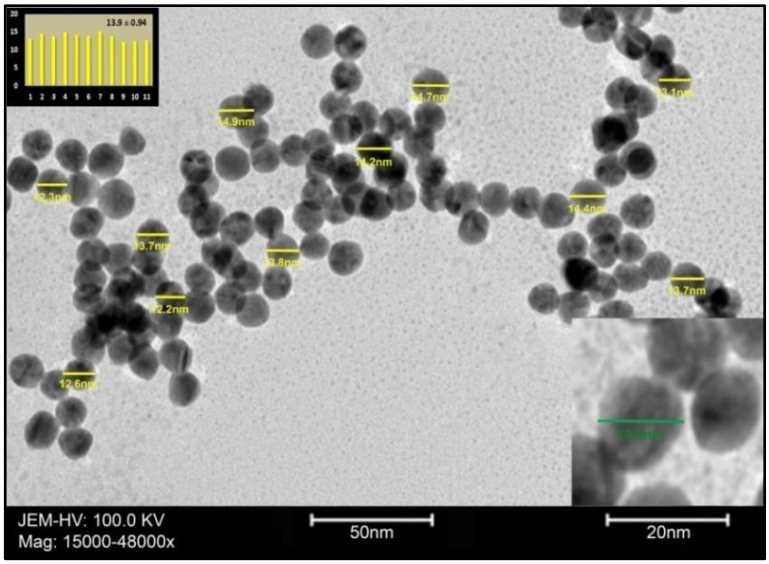

Figure 1: TEM micrograph displaying the surface morphology, particle diameter, distribution and the aggregation status of ultrasonicated Ag-NPs.

Matrix Metalloproteinases concentrations

The one-way ANOVA demonstrated that the administered dose of Ag-NPs at the different exposure levels (0.0, 0.5% and recovery) for a time of 7 days had no significant effect on the skin MMP-2 concentration. Tukey HSD and Games-Howell tests revealed a highly significant increase in the of skin MMP-2 in group II and III over the control (group I), after 14 days of experimental period. On the other hand, significantly elevated concentrations of

Article DOI: 10.52589/AJBMR-QMDCSAYF
DOI URL: https://doi.org/10.52589/AJBMR-QMDCSAYF

skin MMP-9 were exhibited in all the studied groups, at the end of both exposure periods. The highest percentage of change for both MMPs was recorded in the skin of the exposure rabbits (group II), whereas the concentrations after recovery (group III) were significantly decreased, but still higher than that of the controls. MMP-9 was the most affected enzyme and MMP-2 showed the minimal effect (Table 3).

Table 3: The concentrations of MMP-2 and MMP-9 (ng/g wt) in the rabbit skin after 7 and 14 days of sub-acute exposure to 0.5% Ag-NPs. Data are represented as a mean ± SEM.

Parameter	Periods	Group I	Group II	Group III
MMP-2	7 days	5.62±0.05	5.71±0.01	5.67±0.02
	14 days	5.59±0.06	7.16±0.02 (+28%) ^{A}	6.58±0.03 (+19%) ^{AB}
MMP-9	7 days	49.18±0.15	57.24±0.44 (+16%) ^{A}	51.45±0.61 (+5%) ^{AB}
	14 days	49.17±0.21	88.43±0.26 (+79%) ^{A}	72.64±0.31 (+48%) ^{AB}

(A) and (B): In the same row, indicated a significant difference ($P<0.05$) in comparison with groups I and II respectively, as demonstrated by ANOVA.

Gene Expression Analysis of Matrix Metalloproteinases

RNA Quantification and Quality Control

The Spectrophotometeric calculated ratios of absorbance at 260 nm to the absorbance of proteins (A260/A280) and other contaminants (A260/A230) were found in the range of typical requirements; 1.8–2.2 and >1.7 respectively, which evidently indicated the purity of RNA samples at the different exposure levels and experimental periods (Table 4).

Table 4: The quantitative and quality control analysis data of the extracted RNA from the skin of rabbits exposed to sub-acute dose of 0.5% Ag-NPs.

Parameter	Group I (Control)		Group II (Exposure)		Group III (Recovery)	
Exposure Periods	7 days	14 days	7 days	14 days	7 days	14 days
RNA (µg/ml)	70.67	71.94	71.74	70.75	72.11	75.19
$A_{260/280}$	2.09	2.07	2.01	1.99	2.04	2.01
$A_{260/230}$	2.01	1.98	1.99	1.97	2.01	1.98
28S/18S	2.06	2.02	2.01	2.08	2.03	2.12

Additionally, the high qualities of the isolated RNA was confirmed by the formaldehyde agarose (FA) gel electrophoresis where the staining intensity ratio of 28S:18S rRNA bands of all samples was higher than 2:1 and the major ribosomal RNA bands (28S and 18S) were clearly identified without any degradation products (Table 4 and Figure 2).

Article DOI: 10.52589/AJBMR-QMDCSAYF
DOI URL: https://doi.org/10.52589/AJBMR-QMDCSAYF

African Journal of Biology and Medical Research
ISSN: 2689-534X
Volume 4, Issue 4, 2021 (pp. 8-21)

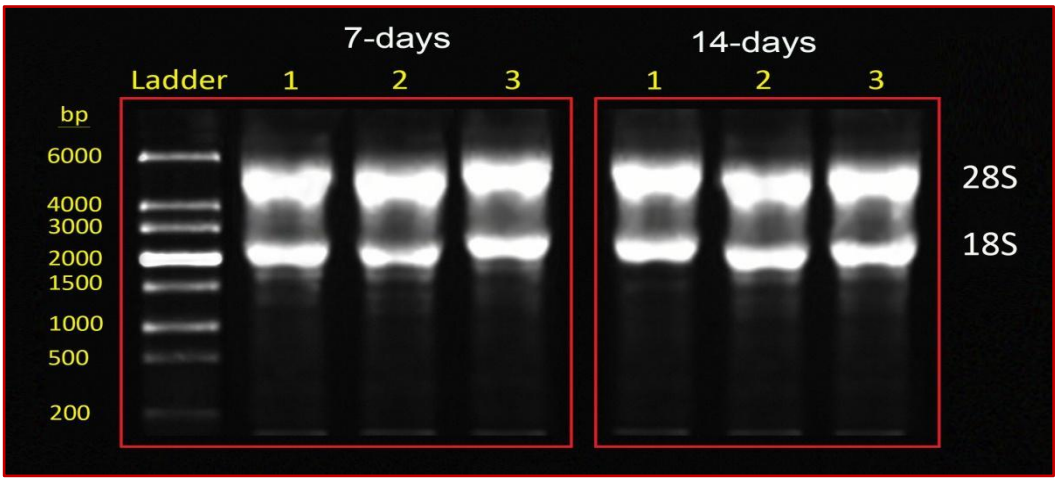

Figure 2: FA gel electrophoresis: showing the ethidium bromide-staining pattern of intact total RNA extracted from the skin of control rabbits (group I/ lane 1), those exposed to 0.5% Ag-NPs after 7 and 14 days of exposure (group II/ lane 2), and the recovery levels after 7 days from the end of the exposure period (group III/ lane 3). The clearly defined 18S and 28S ribosomal RNA bands appear and the purity of total RNAs was approved.

RT-PCR and Relative Gene Expressions

The ethidium bromide-stained agarose gel demonstrated that the PCR amplification of GAPDH produced a cDNA of the expected size. Besides, the homogeneity of the electrophorized PCR band intensities verified the stable expression of GAPDH gene in all skin samples. The amplification of MMP-2 and MMP-9 specific mRNA verified the gene expression of these MMPs in the skin of rabbits at the different exposure levels (0.0, 0.5% and recovery) and periods (7 and 14 days) of sub-acute exposure to 0.5% Ag-NPs. Both MMP-1 and MMP-9 mRNA expression bands were clearly identified at the expected size without any other contaminants. In addition, no significant change was recorded neither in MMP-2 nor in MMP-9 band intensities between all studied groups after 7 days of sub-acute exposure to 0.5% Ag-NPs. Conversely, the skin of exposure (group II) and recovery (group III) rabbits showed an increased band intensity of both MMPs when compared with that of the controls (group I), after the 14 days experimental period (Figure 3).

Article DOI: 10.52589/AJBMR-QMDCSAYF
DOI URL: https://doi.org/10.52589/AJBMR-QMDCSAYF

African Journal of Biology and Medical Research
ISSN: 2689-534X
Volume 4, Issue 4, 2021 (pp. 8-21)

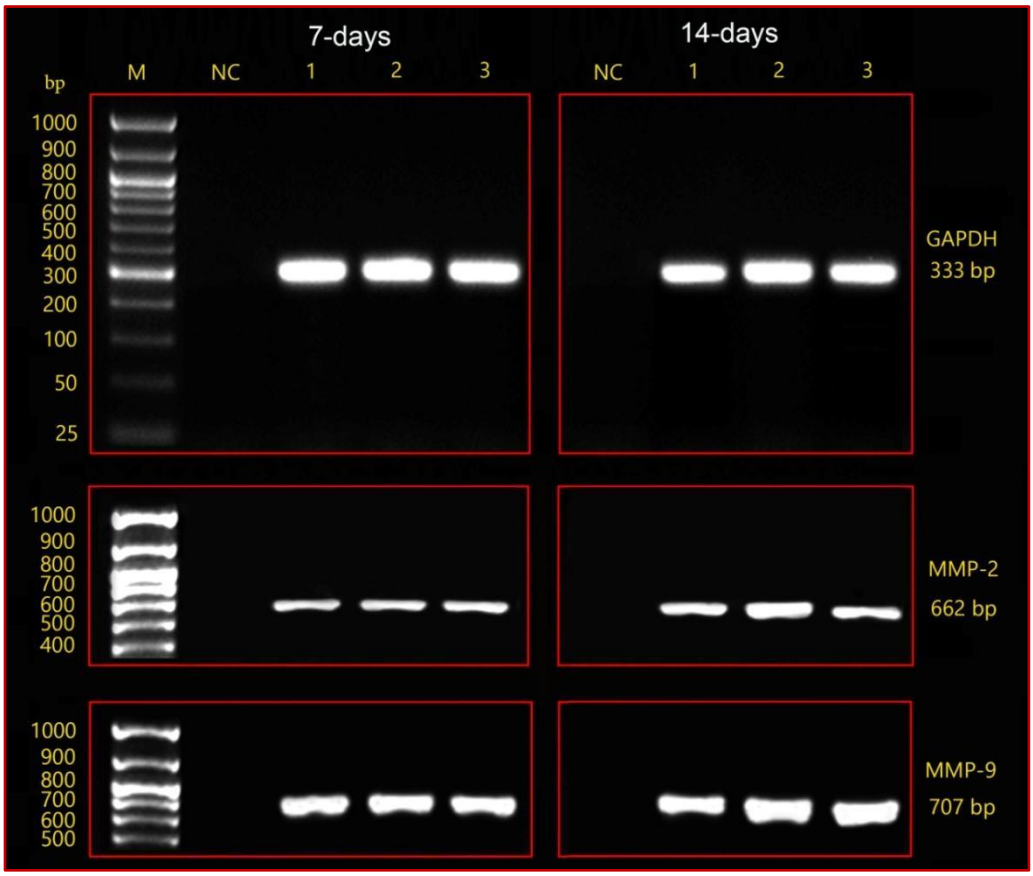

Figure 3. Ethidium bromide-stained agarose gel showing RT-PCR products that encode the expression level of GAPDH, MMP-2 and MMP-9 in the skin of sub-acute experimental rabbits exposed to an every other day dose of (0% and 0.5%) Ag-NPs, after 7 and 14 days of exposure. M indicates DNA ladder as a size marker; NC for negative PCR control without sample; Lane-1 for the control rabbits (group I); Lane-2 for the exposure (group II); and Lane-3 represents the recovery rabbits (group III).

The one-way analysis of variance with Duncan's test of homogeneity revealed that the relative gene expressions of MMP-2 and MMP-9 after normalization to GAPDH were insignificantly affected by the different levels of Ag-NPs at the exposure time of 7 day. Whereas highly significant increase in the expression levels was observed in groups II and III, respectively when compared with that of the control in group I, after the 14 days experimental period. The skin of exposed rabbits (group II) showed the maximum relative gene expression of MMPs, whereas the recovery rabbits (group III) showed significantly decreased expression levels, but still significantly higher than the mean value of the controls in group I (Tables 5).

Article DOI: 10.52589/AJBMR-QMDCSAYF
DOI URL: https://doi.org/10.52589/AJBMR-QMDCSAYF

Table 5: The quantification of MMP-2 and MMP-9 relative gene expressions as normalized to GAPDH in the skin of rabbits after 7 and 14 days of sub-acute exposure to 0.5% of Ag-NPs. Data are represented as a mean ± SEM.

Parameter	Experimental Periods	Group I (control)	Group II (exposure)	Group III (recovery)
MMP-2	7 days	0.36±0.005	0.36±0.004	0.36±0.002
	14 days	0.36±0.004	0.43±0.005 (+19%) ^{A}	0.41±0.002 (+14%) ^{AB}
MMP-9	7 days	0.71±0.005	0.71±0.004	0.71±0.002
	14 days	0.71±0.004	0.85±0.005 (+20%) ^{A}	0.79±0.002 (+11%) ^{AB}

(A) and (B): In the same row, indicated a significant difference ($P<0.05$) in comparison with groups I and II respectively, as demonstrated by ANOVA.

DISCUSSION

The role of MMPs is of special interest in the wound healing process which has been proven to be accelerated in the presence of Ag-NPs. Controlling expression, levels, and activities of these proteolytic enzymes in the skin could be a possible way for understanding their role in wound healing. The present results indicate that 7 days of exposure to sub-acute dose of 0.5% Ag-NPs had no significant effect neither on the level nor the on the expression of MMP-2 among all rabbits under investigation. On the other hand, a significant increase in MMP-9 was recorded only in the enzyme level, whereas there was no effect in the expression of this protein in both the exposure and the recovery groups.

These results are in accordance with the fact that the production level of MMPs is controlled by several regulatory mechanisms that may interact with each other. MMPs are secreted from cells as a latent zymogen which in turn transforms into the final active form. The activation process can be restricted in several ways including, the zinc chelating agents that have the ability to invade the enzyme active center and replaces zinc-bond by their ions (Cui *et al*., 2017). Accordingly, the alteration in MMP-9 level found herein most likely reflects the role of silver ions release in the transition of latent zymogen to the active final form of enzyme (Fajar *et al*., 2019).

Our results also revealed that the levels of both MMP-2 and MMP-9 were significantly up-regulated in the skin of exposed and recovered rabbits over the normal values of control, at the 14 days experimental period. In addition, the expressions of these MMPs encoding genes were also increased at the transcriptional level. That effect was indicated through the increased band density as well as up-regulated relative gene expression of mRNA. Collectively, these results revealed that the effect of Ag-NPs on the MMPs gene expression is time dependent and 7 days of exposure were not long enough to alter MMPs expression and production.

Previous studies have investigated the effect of Ag-NPs on MMPs levels, activities and gene expressions *in vitro*. Basically, oxidative stress has been found as the main pathway for

Article DOI: 10.52589/AJBMR-QMDCSAYF
DOI URL: https://doi.org/10.52589/AJBMR-QMDCSAYF

MMPs activation and production following the release of ROS in response to silver exposure (Samberg *et al*., 2010; Vila *et al*., 2017). Consequently, the activation of MMPs seems to be directly correlated with the excessive ROS production (Wan *et al*., 2008).

In support of this assumption, Inkielewicz- Stępniak *et al*. (2014) showed that the significant increase in MMP9 mRNA expression and the final enzyme activity was mainly dependent on the initiated oxidative stress in human gingival fibroblasts exposed to Ag-NPs, including the release of excessive ROS and elevated proinflammatory cytokines level. Similarly, an increased MMP9 protein concentration and enzyme activity following the exposure to Ag-NPs, was recorded through ROS generation pathway in different cell lines such as, human bronchial epithelial cells (Choo *et al*., 2016), rat embryonic cells (Xu *et al*., 2015), and in the primary porcine brain capillary endothelial cells (Cramer *et al*., 2014).

Another possible interpretation relies on the fact that bio-activities of most metallic NPs are reported to be associated with impaired phagocytosis, temporary inflammation, releasing inflammatory cytokines and inhibiting their functions (Monteiro-Riviere *et al*., 2005; Soto *et al*., 2007). An early study documented that NPs have the ability to modulate MMPs at both the cellular and transcriptional levels, partly through TNF-α and IL-1β dependent pathways (Armand *et al*., 2013).

CONCLUSION

The current study highlights the effect of Ag-NPs on the most prominent skin MMPs. The regulatory action of these nanoparticles was suggested to be a result of interference of more than one pathway. Each suggestion requires further molecular studies to gain more evidence about the most probable mechanism to explain that effect which might be useful for the development of more advanced and efficient medical products.

REFERENCES

Armand, L., Dagouassat, M., Belade, E., Simon-Deckers, A., Le Gouvello, S., Tharabat, C., Duprez, C., Andujar, P., Pairon, J. C., Boczkowski, J., & Lanone, S. (2013). Titanium dioxide nanoparticles induce matrix metalloprotease 1 in human pulmonary fibroblasts partly via an interleukin-1β-dependent mechanism. American journal of respiratory cell and molecular biology., 48(3), 354–363.

Caroline, J. (2002): Quantitative Reverse Transcription-PCR. RT-PCR Protocols. Methodology of Molecular biology., 193, 89603-875.

Choo, W. H., Park, C. H., Jung, S. E., Moon, B., Ahn, H., Ryu, J. S., Kim, K. S., Lee, Y. H., Yu, I. J., & Oh, S. M. (2016). Long-term exposures to low doses of silver nanoparticles enhanced in vitro malignant cell transformation in non-tumorigenic BEAS-2B cells. Toxicology in vitro: an international journal published in association with BIBRA, 37, 41–49.

Cramer, S., Tacke, S., Bornhorst, J., Klingauf, J., Schwerdtle, T., &Galla, H.J. (2014). The influence of silver nanoparticles on the blood-brain and the blood-cerebrospinal fluid barrier in vitro. Journal of Nanomedicine & Nanotechnology, 5, 225-233.

Article DOI: 10.52589/AJBMR-QMDCSAYF
DOI URL: https://doi.org/10.52589/AJBMR-QMDCSAYF

Cui, N., Hu, M., & Khalil, R. A. (2017). Biochemical and Biological Attributes of Matrix Metalloproteinases. Progress in molecular biology and translational science, 147, 1–73.
El-Rafie, H., El-Rafie, M., & Zahran, M. (2017). Anti-Inflammatory and Antibacterial Activities of Nanosilver-Treated Cotton Fabric Prepared from Ethanolic Extracts of Three Terminalia Species. Egyptian Journal of Chemistry, 60, 129-142.
Fajar, M.N., Endarko, E., Rubiyanto, A., Malek, N., Hadibarata, T. and Syafiuddin, A. (2019). A green deposition method of silver nanoparticles on textiles and their antifungal activity. Biointerface Research in Applied. Chemistry, 10, 4902-4907.
Gou, X., Xue, Y., Zheng, H., Yang, G., Chen, S., Chen, Z., & Yuan, G. (2020). Gelatinases Cleave Dentin Sialoprotein Intracellularly. Frontiers in physiology, 11, 686-698.
Hrabia A. (2021). Matrix Metalloproteinases (MMPs) and Inhibitors of MMPs in the Avian Reproductive System: An Overview. International journal of molecular sciences, 22(15), 8056.
Inkielewicz-Stepniak, I., Santos-Martinez, M. J., Medina, C., & Radomski, M. W. (2014). Pharmacological and toxicological effects of co-exposure of human gingival fibroblasts to silver nanoparticles and sodium fluoride. International journal of nanomedicine, 9, 1677–1687.
Janssens, N., Janicot, M., Perera, T., & Bakker, A. (2004). Housekeeping genes as internal standards in cancer research. Molecular diagnosis Journal, 8(2), 107–113.
Koduru, J. R., Kailasa, S. K., Bhamore, J. R., Kim, K. H., Dutta, T., & Vellingiri, K. (2018). Phytochemical-assisted synthetic approaches for silver nanoparticles antimicrobial applications: A review. Advances in colloid and interface science, 256, 326–339.
Korani, M., Rezayat, S. M., & Arbabi Bidgoli, S. (2013). Sub-chronic Dermal Toxicity of Silver Nanoparticles in Guinea Pig: Special Emphasis to Heart, Bone and Kidney Toxicities. Iranian journal of pharmaceutical research, 12(3), 511–519.
Korani, M., Rezayat, S. M., Gilani, K., Arbabi Bidgoli, S., & Adeli, S. (2011). Acute and subchronic dermal toxicity of nanosilver in guinea pig. International journal of nanomedicine, 6, 855–862.
Lee, S. H., & Jun, B. H. (2019). Silver Nanoparticles: Synthesis and Application for Nanomedicine. International journal of molecular sciences, 20(4), 865-879.
Mikhailova E. O. (2020). Silver Nanoparticles: Mechanism of Action and Probable Bio-Application. Journal of functional biomaterials, 11(4), 84-109.
Monteiro-Riviere, N. A., Nemanich, R. J., Inman, A. O., Wang, Y. Y., & Riviere, J. E. (2005). Multi-walled carbon nanotube interactions with human epidermal keratinocytes. Toxicology letters, 155(3), 377–384.
Mussin, J. E., Roldán, M. V., Rojas, F., Sosa, M., Pellegri, N., & Giusiano, G. (2019). Antifungal activity of silver nanoparticles in combination with ketoconazole against Malassezia furfur. AMB Express, 9(1), 131-155.
Negut, I., Grumezescu, V., & Grumezescu, A. M. (2018). Treatment Strategies for Infected Wounds. Molecules (Basel, Switzerland), 23(9), 2392.
NRC, National Research Council. (2011). Guide for the Care and Use of Laboratory Animals, 8th ed. National Academies Press.
Nyman, J. S., Lynch, C. C., Perrien, D. S., Thiolloy, S., O'Quinn, E. C., Patil, C. A., Bi, X., Pharr, G. M., Mahadevan-Jansen, A., & Mundy, G. R. (2011). Differential effects between the loss of MMP-2 and MMP-9 on structural and tissue-level properties of bone. Journal of bone and mineral research: the official journal of the American Society for Bone and Mineral Research, 26(6), 1252–1260.

Article DOI: 10.52589/AJBMR-QMDCSAYF
DOI URL: https://doi.org/10.52589/AJBMR-QMDCSAYF

Paladini, F., & Pollini, M. (2019). Antimicrobial Silver Nanoparticles for Wound Healing Application: Progress and Future Trends. Materials (Basel, Switzerland), 12(16), 2540.

Panja A, Mishra A, Dash M, Pandey N, Singh S, Kumar B. (2021). Silver Nanoparticles – A Review. Eorasian Journal of Medicine and Oncology.; 5(2): 95-102.

Samberg, M. E., Oldenburg, S. J., & Monteiro-Riviere, N. A. (2010). Evaluation of silver nanoparticle toxicity in skin in vivo and keratinocytes in vitro. Environmental health perspectives, 118(3), 407–413.

Shapiro, S. S., & Wilk, M. B. (1965). An Analysis of Variance Test for Normality (Complete Samples). Biometrika, 52(3/4), 591–611.

Soto, K., Garza, K. M., & Murr, L. E. (2007). Cytotoxic effects of aggregated nanomaterials. Acta biomaterialia, 3(3), 351–358.

Velnar, T., & Gradisnik, L. (2018). Tissue Augmentation in Wound Healing: The Role of Endothelial and Epithelial Cells. Medical archives, 72(6), 444–448.

Vila, L., Marcos, R., & Hernández, A. (2017). Long-term effects of silver nanoparticles in caco-2 cells. Nanotoxicology, 11(6), 771–780.

Wan, R., Mo, Y., Zhang, X., Chien, S., Tollerud, D. J., & Zhang, Q. (2008). Matrix metalloproteinase-2 and -9 are induced differently by metal nanoparticles in human monocytes: The role of oxidative stress and protein tyrosine kinase activation. Toxicology and applied pharmacology, 233(2), 276–285.

Xu, L., Shi, C., Shao, A., Li, X., Cheng, X., Ding, R., Wu, G., & Chou, L. L. (2015). Toxic responses in rat embryonic cells to silver nanoparticles and released silver ions as analyzed via gene expression profiles and transmission electron microscopy. Nanotoxicology, 9(4), 513–522.

Yin, I. X., Zhang, J., Zhao, I. S., Mei, M. L., Li, Q., & Chu, C. H. (2020). The Antibacterial Mechanism of Silver Nanoparticles and Its Application in Dentistry. International journal of nanomedicine, 15, 2555–2562.

Article DOI: 10.52589/AJBMR-QMDCSAYF
DOI URL: https://doi.org/10.52589/AJBMR-QMDCSAYF